Adsorption of copper ions from water onto fish scales derived biochar: Isothermal perspectives

G.O. Achieng [1*], V.O. Shikuku [2]

[1]*Department of Chemistry, Maseno University, P.O. Box 333-40105, Maseno, Kenya*
[2]*Department of Physical Sciences, Kaimosi Friends University College, P.O. Box 385-50309 Kaimosi-Kenya*

Abstract

In this work, Tilapia (*Oreochromis niloticus*) fish scales were used for the development of an economical biochar (FSB) by slow pyrolysis at 600 ºC. The FSB was characterized using energy dispersive x-ray (EDX), x-ray fluorescence (XRF), x-ray diffractometry (XRD), Fourier transform infrared (FTIR), and scanning electron microscopy (SEM) techniques. The potential of FSB for the uptake of copper ions from water was examined as a function of initial concentration. Adsorption data were treated using eleven adsorption isotherms, and the most applicable equation obtained by comparison of the coefficient of determination (R^2) values calculated by nonlinear regression method. Equilibrium data were best explained by Langmuir isotherm denoting monolayer adsorption of Cu(II) ions onto FSB. The FSB's maximum adsorption capacity was 39.39 mg/g.

1. Introduction

Untreated industrial effluents are known sources of heavy metals loading into surface waters and other environmental compartments [1]. These heavy metals are toxic, at concentrations above certain limits, and disrupt specific biological processes in human beings other living organisms [2]. Copper finds extensive use in various industrial processes such as plating, mining and smelting, electroplating industries, petroleum refining, and Cu-based agrichemicals mining [2]. Effluents from such industries contain considerably high levels of Cu(II) ions, and subsequent use of the polluted wastewater for agricultural purposes introduces the heavy metal into the food chain [3]. In humans, acute copper poisoning has been shown to cause hemolysis, liver, and kidney damage among other disorders. Therefore, proper treatment of effluent before discharge for the removal of heavy metals, such as copper, is essential for environmental health [4].

Several techniques for sequestering heavy metals from water are in use. These include adsorption, biosorption, reverse osmosis, ion exchange, and filtration, among others [5, 6]. Adsorption remains the widely used technique for sequestration of heavy metals from water owing to its efficiency and inherent low-cost in terms of capital investment. Therefore, a suitable adsorbent must be assessed in terms of surface area, pollutant removal efficiency, life-cycle, and cost of production [7]. Over the years, studies have proposed various naturally occurring inorganic materials and agricultural wastes biomass as

low-cost precursor substrates for developing adsorbents for the uptake of metal ions from water. These include Tunisian date stones [8], rice husk [9], cassava peel [10], grape seeds [11], orange peels [12], Jatropha curcas seeds [13], longan seed [14], mung bean husk [15], almond shell [16], corncob [17], peanut hull [18], barley husks [19], solid palm waste [20], bamboo culms [21], grape waste [22] and palm kernel shell [23]. Fish scales are generally considered of no economic value and present an environmental menace if not correctly disposed of. A report by Rustad [24] indicated that approximately 91 million tons of fish and shellfish are captured yearly worldwide, among which about 60 % serves as food for humans, and the remaining percent disposed as waste. Besides, sustainable availability of fish scales as a resource for the production of commercial adsorbents has been supported by statistics in which there was a non-significant change in the amount of fish captured in the face of rising human population [25].

Several works reported the utility of fish scales as adsorbents in the elimination of copper ions from aqueous solution [26], chromium (VI) from industrial effluents [27] and metal ions from wastewater [28]. Other studies on the use of fish scales for sequestration of heavy metals such as Cu, Zn, Fe, Ni, and Mn are also in the literature [29-31]. Recently, Achieng *et al*. [32] reported fish scale derived biochar for the uptake of indigo carmine from water. However, presently, there is no published work on the use of fish scale biochar for the uptake of copper ions from aqueous media.

This work aimed to convert the fish scales, an environmental menace in Gikomba, the largest open market in Nairobi-Kenya, into biochar, a functionalized adsorbent, and to investigate its performance for removal of copper ions from synthetic wastewater. The prepared biochar was characterized using the elemental analyzer (x-ray fluorescence-XRF), scanning electron microscopy (SEM), X-ray diffraction (XRD) and Fourier transform infrared (FTIR) spectroscopy. The equilibrium data were modeled using six two-parameter adsorption isotherm models, namely; Langmuir, Freundlich, Temkin, Fowler-Guggenheim, Elovich, and Flory-Huggins and five three-parameter isotherms, namely; Hill, Sips, Toth, Redlich-Peterson and Koble-Corrigan and the parameters determined using the nonlinear regression method.

2. Material and Methods
2.1 Adsorbent preparation
The *Oreochromis niloticus* (Tilapia) fish scales were obtained at Gikomba market in Nairobi, Kenya. The scales were washed in running tap water to remove adhering dirt, rinsed severally using de-ionized water, air-dried under shade for 3 days, and then heated at 30 $^{\circ}$C. The fish scale biochar (FSB) was then prepared by slow-pyrolysis at 600 $^{\circ}$C as described by Achieng *et al*. [32] with no modifications. The as-prepared adsorbent was stored in airtight glass for characterization and application in the adsorption experiments.

2.2 Characterization of FSB
The functional groups analysis was done using FTIR (ATR-FTIR) equipment. The elemental composition of the fish scale biochar (FSB) was determined by XRF (XRF76V-WRO1) analysis. The mineralogical composition was determined using an X-ray Brucker diffractometer (D8 Advance) with copper radiation ($K_\alpha = 1.5406$).

2.3 Adsorption experiments
During the experiment, 0.1 g FSB samples were shaken in 50 mL solutions, containing different concentrations of Cu^{2+} ions (40, 60, 80, 100, 120, 140, 160, 180 and 200 mg/L) at room temperature without pH adjustment. The solution pH for copper solutions was 5.8±0.2. After 24 h equilibration time, the contents were shaken for 10 min, and the supernatant solution filtered through 0.45 µm diameter

filters. The filtrate was analyzed for residual metal ion content using the Atomic Absorption Spectrophotometer (AAS) instrument with a graphite furnace (Model Number: AA320N, China).

The amount (q_e) of metal ion adsorbed onto FSB was determined using the equation:

$$q_e = \frac{(C_i - C_e)V}{m} \tag{1}$$

The amount of metal ion removed, as a percentage (%), was computed using the relation:

$$metal\ adsorbed(\%) = \frac{(C_i - C_e)}{C_i} \times 100 \tag{2}$$

Where C_i is the initial metal ion concentration, C_e the equilibrium metal ion concentration in the solution (mg L^{-1}), V is solution volume (L), and m is the mass of the FSB used (g).

3. Results and discussion

3.1 Elemental composition
The elemental composition of the fish scale biochar (FSB) obtained by EDX and XRF analysis, as also reported in previous work, is presented in Table 1 [32].

Table 1: Elemental constituents of the FSB

Element	C	N	H	O	Ca	P	Mg	Na
% composition	18.41	0.37	0.06	4 3.74	29.08	13.89	0.46	0.32

3.2 Morphological inspection
The surface morphology of FSB was inspected using the scanning electron microscopy (SEM) and the SEM micrograph is displayed in Figure 1. The micrograph depicts the FSB surface as heterogeneous with unevenly distributed cavities and openings.
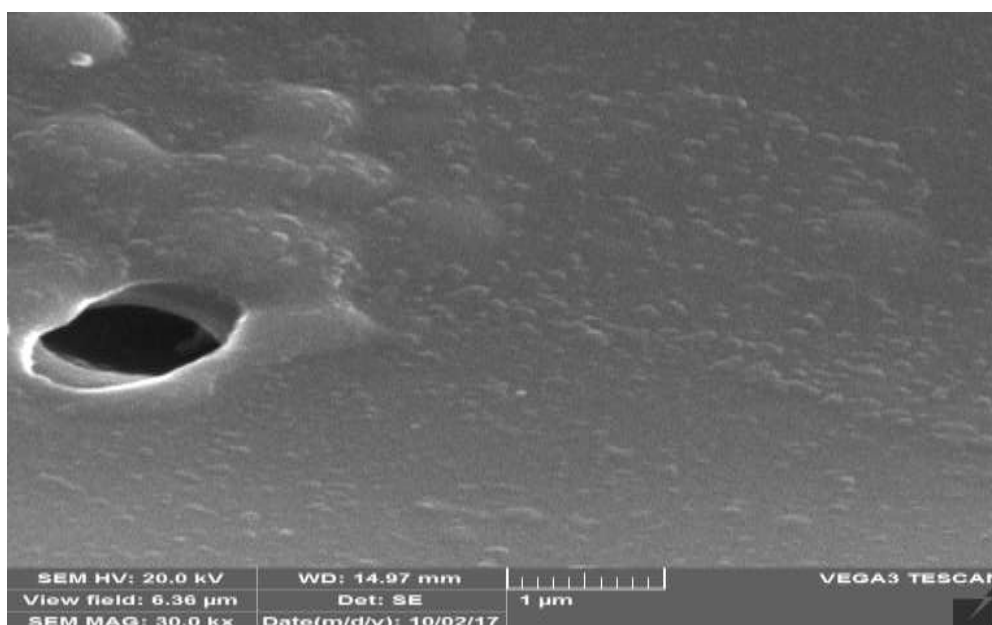

Figure 1: SEM micrograph of FSB

3.3 Crystallinity analysis

Powder x-ray diffraction (PXRD) analysis (Figure 2) was performed to determine the crystallinity and mineral phases in FSB. The fish scale biochar was amorphous with presence of hydroxyl apatite detected.
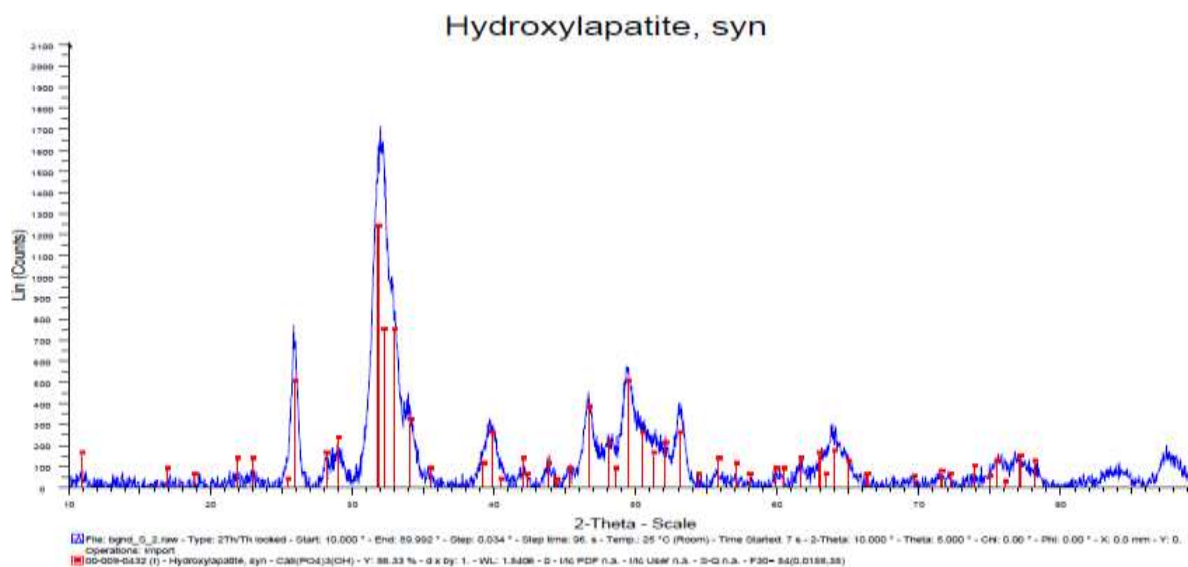

Figure 2: The X-ray diffractogram for fish scale biochar (FSB) adsorbent

3.4 Functional group analysis

Figure 3 shows the FTIR spectrum of FSB. The bands around 3600-3300 cm^{-1} were attributed to –OH stretching vibrations. The bands centered in the region 1700-1600 cm^{-1} were due to C=O stretching vibrations [33]. The 1500-1400 cm^{-1} bands depicted the presence of inorganic functional groups such as alumina-silicates and metal oxides [34, 35].
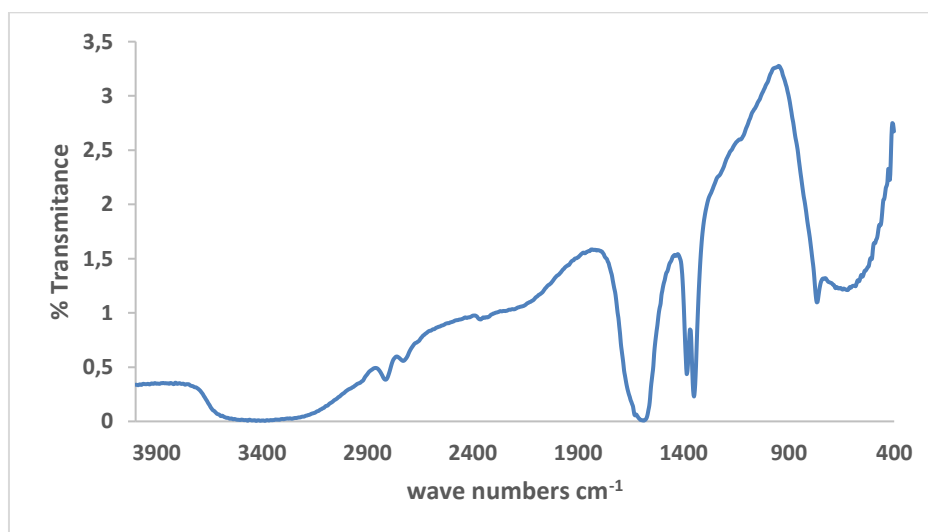

Figure 3: FTIR spectra of fish scale biochar (FSB)

3.5 Two-parameter isotherms

The equilibrium sorption data were modeled using six two-parameter isotherm equations and the best fitting model determined by comparison of the coefficients of determination, R^2. The computed constants are presented in Table 2.

Table 2: Two-parameter isotherm model constants for removal of Cu onto FSB

Isotherm	Langmuir	Freundlich	Temkin	Elovich	Flory-Huggins	Fowler-Guggenheim
Parameter	Q_0= 39.39	K_F=7.42×10^{-9}	B= 4.209	Q_m=2.00×10^5	n= 0.00	W= -3414.3
	K_L= 0.028	1/n= 6.020	A_T=324.59	K_E= 5.15×10^{-7}	K_{FH}= 0.0055	K_{FG}= 0.0029
R^2	0.9999	0.6491	0.9993	0.9485	0.992	0.9524

3.5.1 Langmuir isotherm

Langmuir [36] isotherm assumes a monolayer distribution of adsorbate molecules onto a surface characterized by energetically equivalent binding sites. The nonlinear form of the Langmuir model is given as:

$$q_e = \frac{Q_0 K_L C_e}{1 + K_L C_e} \qquad (4)$$

Where q_e is the number of molecules adsorbed at equilibrium (mg g^{-1}), C_e is the adsorbate concentration in the solution at equilibrium (mg L^{-1}), Q_0 is the theoretical maximum adsorption capacity (mg g^{-1}), and K_L is the Langmuir constant (L g^{-1}).

In this study, the Langmuir model afforded a coefficient of determination, R^2, closest to unity with maximum theoretical adsorption density of 39.39 mg g^{-1}. Based on R^2 values, the Langmuir model best modeled the equilibrium data for Cu abstraction by FSB, suggesting monolayer adsorption.

3.5.2 Freundlich isotherm

Freundlich [37] derived an equation that postulated a multilayer adsorption mechanism onto energetically different adsorption adsorbent sites. The nonlinear Freundlich equation is given as:

$$q_e = K_F C_e^{1/n} \qquad (5)$$

The magnitude of the factor n is an index of how favorable the adsorption process is [38]. Values of n ranging from 2-10 depict good, 1-2 moderately difficult, and < 1, a reduced adsorptive potential. In this study, the magnitude of n (0.166) (Table 2) suggests reduced adsorption potential. Small magnitudes of 1/n are associated with relatively strong bonds [39]. The calculated 1/n value (6.020), denote weaker adsorbate-adsorbent interactions between Cu and the FSB binding sites. According to Saleh [40], 1/n values above unity, as in adsorption of Cu onto FSB, imply cooperative adsorption. The Freundlich model poorly accounted for the adsorption mechanism of Cu onto FSB relative to the other isotherm models as attested to by the R^2 values. On the contrary, Konan *et al*. [56] showed that Freundlich model described, with good precision, the adsorption of methylene blue dye onto activated carbons made from agricultural waste: *borassus* palm tree and bamboo stems. Assaoui *et al*. [57] also reported that experimental data for the adsorption of fluoride onto sodium bentonite clay fitted Freundlich model.

3.5.3 Temkin isotherm

The Temkin isotherm [41] integrates the effects of adsorbate-adsorbate interactions and postulates that the heat of adsorption (ΔH_{ads}) of the adsorbate in the layer reduces linearly with increase in surface coverage. The model is given as:

$$q_e = B_T \left(A_T C_e \right) \qquad (6)$$

$$B_T = \frac{RT}{b_T} \qquad (7)$$

Adsorption energies ($B_T \ln(A_T)$) in the range of 8–16 kJ mol^{-1} and b_T values above 80 kJ mol^{-1} denote chemisorption mechanisms [42]. From Table 3, the computed value of $B_T \ln(A_T)$ was 0.024 kJ mol^{-1} and a corresponding b_T value of 0.588 kJ mol^{-1}. These low energy values suggest a physisorption interaction between copper ions and the FSB adsorbing sites. Additionally, positive b_T values are associated with thermodynamically exothermic processes [43]. The high R^2 values ascertain the applicability of the Temkin model for predicting copper uptake onto fish scale biochar.

3.5.4 Flory-Huggins isotherm

Flory-Huggins isotherm model [44] is developed using the extent of the surface coverage and can be used to inspect the spontaneity of the adsorption process. The Flory-Huggins isotherm model is given as:

$$\frac{\theta}{C_o} = K_{FH} (1-\theta)^{n_{FH}} \tag{8}$$

$$\theta = 1 - \frac{C_e}{C_o} \tag{9}$$

Where KFH is the Flory-Huggins equilibrium constant [L/mg]. The n_{FH} exponent reflects the number of adsorbate ions fixed on given sites. Further, the Flory-Huggins constant, K_{FH}, is used to calculate Gibbs free energy, an index of reaction spontaneity, using the relation [45]:

$$\Delta G = -RT \ln K_{FH} \tag{10}$$

From Table 2, the calculated n_{FH} value (n=0) implies that no molecule was bound on any adsorption site on the FSB adsorbent. This phenomenon was impractical and, therefore, unaccepted. The observation indicates that the underlying assumptions of the Flowry-Huggins isotherm could not sufficiently predict the adsorption of Cu onto FSB despite affording a coefficient of determination of 1. The negative ΔG value (-12.89 kJ mol^{-1} at 298 K), obtained using the Flory-Huggins equilibrium constant, indicates that the adsorption of Cu onto FSB is a thermodynamically spontaneous and favorable process. Furthermore, the magnitude of the ΔG value, below 20 kJ mol^{-1}, implies a physisorption process. This is in agreement with the conclusions from the Temkin isotherm.

3.5.5 The Fowler-Guggenheim isotherm

The Fowler-Guggenheim isotherm equation [46] incorporates a parameter that accounts for the lateral interaction between the adsorbate species. This model is expressed as:

$$C_e = \frac{\theta_{FG}}{K_{FG}(1-\theta_{FG})} \exp\left(\frac{2\theta_{FG}W}{RT}\right) \tag{11}$$

where K_{FG} is the Fowler–Guggenheim equilibrium constant (L mg^{-1}), θ the fractional coverage, R the universal gas constant (kJ mol^{-1} K^{-1}), T the temperature (K), and W is the interaction energy between adsorbed molecules (kJ mol^{-1}).

According to the model, when W>0, the interaction between the adsorbed molecules is attractive. On the contrary, when W<0, the interaction between adsorbed molecules is repulsive, and the heat of adsorption decreases with loading. However, when there is no interaction between adsorbed molecules, then W=0. From Table 3, the calculated value of W was negative, indicating repulsion between the adsorbed Cu ions. From the R^2 value, the Fowler–Guggenheim isotherm favorably described the adsorption of Cu onto FSB.

3.5.6 Elovich isotherm

The Elovich isotherm model [47] postulates that the adsorption sites increase exponentially with adsorption. This isotherm is expressed as:

$$C_e = \frac{q_e}{q_{mE} K_E \exp\left(\frac{-q_e}{q_{mE}}\right)} \tag{12}$$

where K_E is the Elovich equilibrium constant (L mg^{-1}), and q_{mE} is the Elovich maximum adsorption capacity (mg g^{-1}).

Based on R^2 values, the Elovich isotherm poorly described the empirical data but better than the Freundlich isotherm. The predicted Elovich maximum adsorption capacity of FSB for copper removal was 2.00×10^5 mg g^{-1}. However, based on R^2 values, the Langmuir model best accounted for equilibrium data and hence was used to predict the FSB maximum adsorption capacity. The two-parameter adsorption isotherms described the empirical data in the sequence Langmuir > Temkin > Flory-Huggins > Fowler-Guggenheim > Elovich > Freundlich model. Ugbe and Abdus-Salam [58] reported a better Elovich fitting (R^2=0.9717) for methylene blue (MB) and eosin yellow (EY) removal onto natural and synthetic goethite.

3.6 Three-parameter isotherms

The equilibrium sorption data were fitted to five three-parameter isotherm models and the best fitting model and the parameters obtained by the nonlinear regression approach. The calculated parameters are shown in Table 3.

Table 3: Three-parameter isotherm constants for Cu uptake onto FSB

Isotherm	Hill	Sips	Koble-Corrigan	Toth	Redlich-Peterson
Parameters	n_H=2.59	a_s=3.53E-8	A=2.63E-6	z=0.014	g=0
	q_{SH}=296.08	q_{ms}=546.9	B=0.00	q_{mT}=0.015	a_R=0.021
	K_D=89830.7	B_s=3.947	n_K=4.455	a_T=0.00	K_R=1.053
R^2	0.838	0.745	0.708	0.953	0.948

3.6.1 Hill isotherm

The Hill equation [48] postulates the binding of different species onto a homogeneous surface. The model is given as:

$$q_e = \frac{q_{SH} C_e^{n_H}}{K_D + C_e^{n_H}} \tag{13}$$

The Hill isotherm posits that adsorption is a cooperative phenomenon. Accordingly, n_H>1 represents positive cooperativity in binding, n_H=1 denotes non-cooperative binding, while n_H<1 indicates negative cooperativity in binding. In the present work, the Hill isotherm posted an appreciably high R^2 value (0.838), and the calculated n_H value 2.59>1 suggests a positive cooperativity in binding.

3.6.2 Sips isotherm

The Sips isotherm [49] is a combination of both Freundlich and Langmuir models. This model envisions adsorption onto heterogeneous sites where the adsorbate can be fixed onto more than one adsorption site but with no lateral interactions between adsorbed molecules. The Sips isotherm is given as:

$$q_e = \frac{q_{ms} a_s C_e^{B_s}}{1 + a_s C_e^{B_s}} \tag{14}$$

The parameter B_s is the heterogeneity factor. Generally, the higher the magnitude of the constant B_s, the more heterogeneous the system is. When B_s tends to 1, the system's adsorption sites tend towards homogeneity. In this work, the experimental data poorly fitted to the Sips isotherm as reflected by the low

coefficient of determination (R^2=0.745). The magnitude of the constant B_s (3.947) that is above unity denotes heterogeneity of the adsorption surface.

3.6.3 Toth isotherm

The Toth isotherm model [50] was derived to better the fitness of the Langmuir isotherm to empirical data at low and high adsorbate concentrations. The Toth correlation is presented as:

$$q_e = \frac{q_{mT}C_e}{\left(a_T + C_e^z\right)^{1/z}} \tag{15}$$

Parameter z is an index of the system's heterogeneity. The system is perceived to be heterogeneous as z diverges from unity [51]. The Toth isotherm constants are presented in Table 3. The magnitude of z (0.014) was far below unity signifying a heterogeneous adsorption system as predicted by the Sips isotherm. The high coefficient of determination (R^2) value (0.953) indicate the Toth model best fits the experimental data relative to the other models.

3.6.4 Koble-Corrigan isotherm

The Koble-Corrigan isotherm [52] integrates the Langmuir and Freundlich constants and describes heterogeneous adsorption. The model is computed as:

$$q_e = \frac{AC_e^{n_K}}{1 + BC_e^{n_K}} \tag{16}$$

where A, B, and n_K are Koble-Corrigen isotherm constants. In this study, this isotherm was associated with a low R^2 value (0.708) with an n_K constant value of 4.455, greater than unity. Contrarily, Hossain *et al*. [51] reported the uptake of Cu ions onto palm oil fruit shells with n_K values below 1. When the factor n_K is less than 1, the system is said to be heterogeneous [52]. The value reported in this work correspond to homogeneous adsorption surface. Elsewhere, Saadi *et al*. [53] argued that the Kolbe-Corrigan model should be accepted as long as $n_K > 1$, as in this study. Nevertheless, the low R^2 value reveals the inapplicability of the Kolbe-Corrigan equation.

3.6.5 Redlich-Peterson isotherm

The Redlich-Peterson isotherm [54] similarly integrates the Langmuir and the Freundlich isotherm constants, and allows for both homogeneous and heterogeneous adsorption processes. The isotherm is defined as follows:

$$q_e = \frac{K_R C_e}{1 + a_R C_e^g} \tag{17}$$

where K_R (L/g) and a_R (mg L^{-1})$^{-g}$ are the Redlich–Peterson constants and g (dimensionless) is a factor whose magnitude lies between 0 and 1 for heterogeneous sorption [55]. The equation is reduced to the Langmuir model for g=1 and to Henry's law for g=0. In this study, the Redlich-Peterson isotherm posted a relatively high R^2 value (0.948), implying its suitability to describe the experimental data. The calculated g value of zero (0) indicates the system reduces to Henry's law and assumes heterogeneity of the sorption system [55]. However, despite the high R^2 value, the extremely low predicted maximum adsorption capacity (1.053 mg g^{-1}) incoherent with the equilibrium data denotes the unsuitability of the Redlich–Peterson model to describe copper uptake onto FSB. Contrarily, the model was reported as applicable for copper sorption onto palm oil fruit shells [51].

Conclusion

Tilapia (*Oreochromis niloticus*) fish scales, an abundant, unutilized waste, were used as a precursor for the development of biochar (FSB) by slow pyrolysis at $600\,^{\circ}\text{C}$. The synthesized FSB was used as a sorbent to abstract copper ions, a typical toxic heavy metal, from aqueous solution. The isothermal data was tested against two-parameter (Langmuir, Freundlich, Temkin, Elovich, Flory-Huggins, and Fowler-Guggenheim models) and three-parameter (Sips, Hill, Koble-Corrigan, Toth, and Redlich-Peterson) adsorption isotherms. The equilibrium data were best explained by the Langmuir isotherm denoting monolayer adsorption of Cu(II) ions onto FSB with a maximum adsorption capacity of 39.39 mg/g.

References

1. H. Aydın, Y. Bulut, Ç. Yerlikaya, Removal of copper (II) from aqueous solution by adsorption onto low-cost adsorbents, *J. environ. Manage.* 87(1) (2008) 37-45. https://doi.org/10.1016/j.jenvman.2007.01.005

2. R. Singh, N. Gautam, A. Mishra, R. Gupta, Heavy metals and living systems: An overview, *Indian J. Pharmacol*. 43(3) (2011) 246-253. 10.4103/0253-7613.81505

3. E. Demirbas, N. Dizge, M.T. Sulak, M. Kobya, Adsorption kinetics and equilibrium of copper from aqueous solutions using hazelnut shell activated carbon, *Chem. Eng. J.* 148 (2009) 480–487. https://doi.org/10.1016/j.cej.2008.09.027

4. E. Atangana, Production, disposal, and efficient technique used in the separation of heavy metals from red meat abattoir wastewater, *Environ Sci Pollut Res.* 27 (2020) 9424–9434. https://doi.org/10.1007/s11356-019-06850-z

5. L.C. Staicu, E.D. Van Hullebusch, M.A. Oturan, C.J. Ackerson, P.N. Lens, Removal of colloidal biogenic selenium from wastewater, *Chemosphere*. 125 (2015) 130–138. https://doi.org/10.1016/j.chemosphere.2014.12.018

6. S. K. Shukla, N. R. S. Al Mushaiqri, H. M. Al Subhi, K. Yoo, H. Al Sadeq, Low-cost activated carbon production from organic waste and its utilization for wastewater treatment, *Appl. Water Sci.* 10(2) (2020) 62. https://doi.org/10.1007/s13201-020-1145-z

7. F. Li, K. Shen, X. Long, J. Wen, X. Xie, X. Zeng, Y. Liang, Y. Wei, Z. Lin, W. Huang, R. Zhong, Preparation and characterization of biochars from Eichornia crassipes for cadmium removal in aqueous solutions, *PLoS One*. 11(12) (2016) pp13. https://doi.org/10.1371/journal.pone.0148132

8. F. Bouhamed, Z. Elouear, J. Bouzid, Adsorptive removal of copper (II) from aqueous solutions on activated carbon prepared from Tunisian date stones: equilibrium, kinetics and thermodynamics, *J. Taiwan Inst. Chem. Eng.* 43(5) (2012) 741-749. https://doi.org/10.1016/j.jtice.2012.02.011

9. L. Ding, B. Zou, W. Gao, Q. Liu, Z. Wang, Y. Guo, X. Wang, Y. Liu, Adsorption of Rhodamine-B from aqueous solution using treated rice husk-based activated carbon, *Colloids and Surfaces A: Physicochem. Eng. Aspects*. 446 (2014) 1-7. https://doi.org/10.1016/j.colsurfa.2014.01.030

10. J. C. Moreno-Piraján, L. Giraldo, Adsorption of copper from aqueous solution by activated carbons obtained by pyrolysis of cassava peel, *J. Analyt. Appl. Pyrolysis*. 87(2) (2010) 188-193. https://doi.org/10.1016/j.jaap.2009.12.004

11. M. Al Bahri, L. Calvo, M. A. Gilarranz, J. J. Rodríguez, Activated carbon from grape seeds upon chemical activation with phosphoric acid: Application to the adsorption of diuron from water, *Chem. Eng. J.* 203 (2012) 348-356. https://doi.org/10.1016/j.cej.2012.07.053

12. M. E. Fernandez, G. V. Nunell, P. R. Bonelli, A. L. Cukierman, Activated carbon developed from orange peels: Batch and dynamic competitive adsorption of basic dyes, *Industr. Crops Products*. 62(2014) 437-445. https://doi.org/10.1016/j.indcrop.2014.09.015

13. S. H. Hsu, C. S. Huang, T. W. Chung, S. Gao, Adsorption of chlorinated volatile organic compounds using activated carbon made from Jatropha curcas seeds, *J. Taiwan Inst. Chem. Eng.* 45(5) (2014) 2526-2530. https://doi.org/10.1016/j.jtice.2014.05.028

14. J. Yang, M. Yu, W. Chen, Adsorption of hexavalent chromium from aqueous solution by activated carbon prepared from longan seed, Kinetics, equilibrium and thermodynamics, *J. Ind. Eng. Chem.* 21 (2015) 414-422. https://doi.org/10.1016/j.jiec.2014.02.054

15. S. Mondal, K. Sinha, K. Aikat, G. Halder, Adsorption thermodynamics and kinetics of ranitidine hydrochloride onto superheated steam activated carbon derived from mung bean husk, *J. Environ. Chem. Eng.* 3(1) (2015) 187-195. https://doi.org/10.1016/j.jece.2014.11.021

16. M. de Yuso, B. Rubio, M. T. Izquierdo, Influence of activation atmosphere used in the chemical activation of almond shell on the characteristics and adsorption performance of activated carbons, *Fuel processing technol.* 119 (2014) 74-80. https://doi.org/10.1016/j.fuproc.2013.10.024

17. N. V. Sych, S. I. Trofymenko, O. I. Poddubnaya, M. M. Tsyba, V. I. Sapsay, D. O. Klymchuk, A. M. Puziy, Porous structure and surface chemistry of phosphoric acid activated carbon from corncob, *Appl. Surface Sci.* 261 (2012) 75-82. https://doi.org/10.1016/j.apsusc.2012.07.084

18. Z. Y. Zhong, Q. Yang, X. M. Li, K. Luo, Y. Liu, G. M. Zeng, Preparation of peanut hull-based activated carbon by microwave-induced phosphoric acid activation and its application in Remazol Brilliant Blue R adsorption, *Ind. Crops Prod.* 37(1) (2012) 178-185. https://doi.org/10.1016/j.indcrop.2011.12.015

19. M. Loredo-Cancino, E. Soto-Regalado, F. J. Cerino-Córdova, R. B. García-Reyes, A. M. García-León, M. T. Garza-González, Determining optimal conditions to produce activated carbon from barley husks using single or dual optimization, *Journal of Environmental Management*. 125 (2013) 117-125. https://doi.org/10.1016/j.jenvman.2013.03.028

20. N. S. Nasri, U. D. Hamza, S. N. Ismail, M. M. Ahmed, R. Mohsin, Assessment of porous carbons derived from sustainable palm solid waste for carbon dioxide capture, *J. clean. Prod.* 71 (2014) 148-157. https://doi.org/10.1016/j.jclepro.2013.11.053

21. L. Wang, Application of activated carbon derived from 'waste' bamboo culms for the adsorption of azo disperse dye: Kinetic, equilibrium and thermodynamic studies, *J. Environ. Manage.* 102 (2012) 79-87. https://doi.org/10.1016/j.jenvman.2012.02.019

22. H. Sayğılı, F. Güzel, Y. Önal, Conversion of grape industrial processing waste to activated carbon sorbent and its performance in cationic and anionic dyes adsorption, *J. Clean. Prod.* 93 (2015) 84-93. https://doi.org/10.1016/j.jclepro.2015.01.009

23. Kundu, B. S. Gupta, M. A. Hashim, G. Redzwan, Taguchi optimization approach for production of activated carbon from phosphoric acid impregnated palm kernel shell by microwave heating, *J. clean. prod.* 105 (2015) 420-427. https://doi.org/10.1016/j.jclepro.2014.06.093

24. T. Rustad, Utilization of marine by-products, *Electr. J. Environ. Agri. Food Chem.* 2 (2003) 458–463.

25. Food and Agriculture Organization of the United Nations: The State of World Fisheries and Aquaculture 2018 – Meeting the sustainable development goals. FAO, Rome, Italy (2018).

26. E. Huang, Use of fish scales as biosorbent for the removal of copper in water, *Water Res.* 30 (2007) 1985–1990.

27. S. Bamukyaye, W. Wanasolo, Performance of egg-shell and fish-scale as adsorbent materials for chromium (VI) removal from effluents of tannery industries in Eastern Uganda, *Open Access Library Journal*. 4(8) (2017) 1-12. 10.4236/oalib.1103732

28. J. Villanueva-Espinosa, M. Hernandez-Esparza, F. Ruiz-Trevino, Adsorptive properties of fish scales of *Oreochromis Niloticus* (Mojarra Tilapia) for metallic ion removal from waste water. *Ind. Eng. Chem. Res*. 40 (2001) 3563–3569. https://doi.org/10.1021/ie000884v

29. N. Othman, A. Abd-Kadir, N. Zayadi, Waste fish scale as cost effective adsorbent in removing zinc and ferum ion in wastewater, ARPN *J. Eng. Appl. Sci.* 11 (2016) 1584–1592.

30. Z. Ahmadifar, A. D. Koohi, Characterization, preparation, and uses of nanomagnetic Fe_3O_4 impregnated onto fish scale as more efficient adsorbent for Cu^{2+} ion adsorption, *Environ. Sci.d Pollut. Res.* 25 (2018) 19687–19700. https://doi.org/10.1007/s11356-018-2058-3

31. E. Kwaansa–Ansah, D. Nkrumah, S. Nti, F. Opoku, Adsorption of heavy metals (Cu, Mn, Fe and Ni) from surface water using Oreochromis niloticus scales, *Pollution*. 5 (2019) 115–122.

32. G. O. Achieng', C. O. Kowenje, J. O. Lalah, S. O. Ojwach, Preparation, characterization of fish scales biochar, and their applications in the removal of anionic indigo carmine dye from aqueous solutions, *Water Sci. Technol*. 80(11) (2019) 2218-223. https://doi.org/10.2166/wst.2020.040

33. D. Mohan, A. Sarswat, Y. S. Ok, C. U. Pittman Jr, Organic and inorganic contaminants removal from water with biochar, a renewable, low cost and sustainable adsorbent–a critical review, *Bioresour. Technol.* 160 (2014) 191-202. https://doi.org/10.1016/j.biortech.2014.01.120

34. H. Jin, S. Capareda, Z. Chang, J. Gao, Y. Xu, J. Zhang, Biochar pyrolytically produced from municipal solid wastes for aqueous As (V) removal: adsorption property and its improvement with KOH activation, *Bioresource technology.* 169 (2014) 622-629. https://doi.org/10.1016/j.biortech.2014.06.103

35. S. Soltani, N. Khanian, U. Rashid, T. S. Y. Choong, Fundamentals and recent progress relating to the fabrication, functionalization and characterization of mesostructured materials using diverse synthetic methodologies, *RSC Advances*. 10(28) (2020) 16431-16456. https://doi.org/10.1039/D0RA00440E

36. I. Langmuir, The constitution and fundamental properties of solids and liquids, *J. Am. Chem. Soc*. 38 (1918) 2221–2295. https://doi.org/10.1021/ja02268a002

37. H.M.F. Freundlich, Uber die Adsorption in Losungen, Z. *Phys. Chem.* 57 (1906) 385–470. https://doi.org/10.1515/zpch-1907-5723

38. R.E. Treybal, Mass-transfer Operations, 3rd ed., McGraw-Hill. Using tree fern as a biosorbent, *Process Biochem.* 40 (1981) 119–124.

39. M. H. To, P. Hadi, C. W. Hui, C. S. K. Lin, G. McKay, Mechanistic study of atenolol, acebutolol and sulfamethoxazole adsorption on waste biomass derived activated carbon, *J. Molecular Liquids.* 241 (2017) 386-398. https://doi.org/10.1016/j.molliq.2017.05.037

40. T.A. Saleh, Isotherm, kinetic, and thermodynamics studies on Hg(II) adsorption from aqueous solution by silica-multiwall carbon nanotubes, *Environ. Sci. Pollut. Res*. 22 (2015) 16721–16731. https://doi.org/10.1007/s11356-015-4866-z

41. M.I. Temkin, V. Pyzhev, Kinetics of ammonia synthesis on promoted iron catalyst, *Acta Phys. Chim. USSR.* 12 (1940) 327–356.

42. D. Rahangdale, A. Kumar, Chitosan as a substrate for simultaneous surface imprinting of salicylic acid and cadmium, *Carbohydr. Polymer*. 202 (2018) 334–344. https://doi.org/10.1016/j.carbpol.2018.08.129

43. S. M. Miraboutalebi, S. K. Nikouzad, M. Peydayesh, N. Allahgholi, L. Vafajoo, G. McKayc, Methylene blue adsorption via maize silk powder: Kinetic, equilibrium, thermodynamic studies, and residual error analysis, *Proc. Safety Environ. Prot*. 106 (2017) 191–202. https://doi.org/10.1016/j.psep.2017.01.010

44. M. Horsfall, A.I. Spiff, Equilibrium sorption study of Al^{3+}, Co^{2+} and Ag^{2+} in aqueous solutions by fluted pumpkin (Telfairia occidentalis HOOK) waste biomass, *Acta Chim. Slov*. 52 (2005) 174–181

45. K. Vijayaraghavan, T.V.N. Padmesh, K. Palanivelu, M. Velan, Biosorption of nickel(II) ions onto Sargassum wightii, application of two-parameter and three-parameter isotherm models, *J. Hazard. Mater*. B133 (2006) 304–308. https://doi.org/10.1016/j.jhazmat.2005.10.016

46. R.H. Fowler, E.A. Guggenheim, Statistical Thermodynamics, Cambridge University Press, London. (1939) 431–450.

47. S.Y. Elovich, O.G. Larinov, Theory of adsorption from solutions of non-electrolytes on solid (I) equation adsorption from solutions and the analysis of its simplest form, (II) verification of the equation of adsorption isotherm from solutions, *Izv. Akad. Nauk. SSSR, Otd. Khim. Nauk*. 2 (1962) 209–216.

48. K.Y. Foo, B.H. Hameed, Review: Insights into the modeling of adsorption isotherm systems. *Chem. Eng. J.* 156 (2010) 2–10. https://doi.org/10.1016/j.cej.2009.09.013

49. R.J. Sips, On the structure of a catalyst surface, *J. Chem. Phys*. 16 (1948) 490–495. https://doi.org/10.1063/1.1746922

50. J. Toth, State equations of the solid–gas interface layer, *Acta Chem. Acad. Hung*. 69 (1971) 311–317

51. M.A. Hossain, H.H. Ngo, W.S. Guo, T.V. Nguyen, Palm oil fruit shells as biosorbent for copper removal from water and wastewater: Experiments and sorption models, *Bioresour. Technol.* 113 (2012) 97–101. https://doi.org/10.1016/j.biortech.2011.11.111

52. R.A. Koble, T.E. Corrigan, Sorption isotherms for pure hydrocarbons, *Ind. Eng. Chem*. 44 (1952) 383–387. https://doi.org/10.1021/ie50506a049

53. R. Saadi, Z. Saadi, R. Fazaeli, N.E. Fard, Monolayer and multilayer adsorption isotherm models for sorption from aqueous media, *Korean J. Chem. Eng*. 32(5) (2015) 787-799. https://doi.org/10.1007/s11814-015-0053-7

54. O. Redlich, D.L. Peterson, A useful adsorption isotherm, *J. Phys. Chem*. 63(6) (1959) 1024-1026. https://doi.org/10.1021/j150576a611

55. S.J. Allen, Q. Gan, R. Matthews, P.A. Johnson, Comparison of optimized isotherm models for basic dye adsorption by kudzu, *Bioresour. Technol*. 88 (2003) 143–152. https://doi.org/10.1016/S0960-8524(02)00281-X

56. A. T. S. Konan, R. Richard, C. Andriantsiferana, K. B. Yao, M.-H. Manero, Recovery of *borassus* palm tree and bamboo waste into activated carbon: application to the phenolic compound removal, *J. Mater. Environ. Sci*. 11(10) (2020) 1584-1598.

57. J. Assaoui, A. Kheribech, L. Khamliche, R. Brahmi, Z. Hatim, Study of the adsorption of fluoride in aqueous solution by eco-friendly cost-effective adsorbent: characterization and adsorption mechanism, *Moroccan Journal of Chemistry*. 8 (2020) 1033-1047. https://doi.org/10.48317/IMIST.PRSM/morjchem-v8i4.22364

58. F.A. Ugbe, N. Abdus-Salam, Kinetics and thermodynamic modelling of natural and synthetic goethite for dyes scavenging from aqueous systems, *Arabian Journal of Chemical and Environmental Research*. 7(1) (2020) 12-28